54. IWK

Internationales Wissenschaftliches Kolloquium
International Scientific Colloquium

Information Technology and Electrical Engineering - Devices and Systems, Materials and Technologies for the Future

Faculty of Electrical Engineering and Information Technology

Startseite / Index:
http://www.db-thueringen.de/servlets/DocumentServlet?id=14089

TECHNISCHE UNIVERSITÄT
ILMENAU

Impressum

Herausgeber: Der Rektor der Technischen Universität Ilmenau
Univ.-Prof. Dr. rer. nat. habil. Dr. h. c. Prof. h. c.
Peter Scharff

Redaktion: Referat Marketing
Andrea Schneider

Fakultät für Elektrotechnik und Informationstechnik
Univ.-Prof. Dr.-Ing. Frank Berger

Redaktionsschluss: 17. August 2009

Technische Realisierung (USB-Flash-Ausgabe):
Institut für Medientechnik an der TU Ilmenau
Dipl.-Ing. Christian Weigel
Dipl.-Ing. Helge Drumm

Technische Realisierung (Online-Ausgabe):
Universitätsbibliothek Ilmenau
ilmedia
Postfach 10 05 65
98684 Ilmenau

Verlag:
Verlag ISLE, Betriebsstätte des ISLE e.V.
Werner-von-Siemens-Str. 16
98693 Ilmenau

ISBN (USB-Flash-Ausgabe): 978-3-938843-45-1
ISBN (Druckausgabe der Kurzfassungen): 978-3-938843-44-4

Startseite / Index:
http://www.db-thueringen.de/servlets/DocumentServlet?id=14089

THERMOELECTROMAGNETIC STIRRING IN METALLURGY

A. Cramer, X. Zhang, and G. Gerbeth

Forschungszentrum Dresden-Rossendorf, Dept. of Magnetohydrodynamics,
Bautzner Landstraße 400, PO Box 51 01 19, 01314 Dresden, Germany

ABSTRACT

Thermoelectromagnetic convection in cubic containers was studied experimentally. Two opposing side walls were cooled and heated, respectively, to produce an uniform temperature gradient. Inhomogeneous magnetic field distributions $\vec{B}$ were achieved either with a permanent magnet or with specifically shaped pole shoes of an electromagnetic system. Ultrasonic Doppler velocimetry demonstrated that even a moderate temperature gradient may drive distinct convection. Two different flow regimes were investigated with the permanent magnet. Located at an isothermal wall, it produced a single vortex spreading the whole container while the flow was relatively stable. Moving the magnet to the center altered the flow structure. Four vortices developed and the velocity fluctuations were intensified. The more generic case realised with the electromagnet provided a gradient of $\vec{B}$ only in one direction. Since the field strength and the area of impact on the melt were larger, developed turbulent regimes were accomplished.

Index Terms— Magnetohydrodynamics, Seebeck effect, thermoelectromagnetic convection, metallurgy, stirring

1. INTRODUCTION

The interaction between a thermoelectric current $\vec{j}$ and an imposed magnetic field $\vec{B}$ may produce thermoelectromagnetic convection (TEMC). Prerequisite for $\vec{j}$ is a temperature gradient $\vec{\nabla}T$ and a spatial variation of the thermoelectric power S, both of which in combination may generate an electro-motive force (emf). In his pioneering study [1], Shercliff generalized Ohm's law for conducting liquids by introducing a term for the emf

$$\frac{\vec{j}}{\sigma} = \vec{E} + \vec{v} \times \vec{B} - S \cdot \vec{\nabla}T. \qquad (1)$$

σ, $\vec{v}$, and $\vec{E}$ are electrical conductivity of the liquid metal, velocity at which it moves, and electric field, respectively. In a system in which $\vec{v} \times \vec{B}$ is negligibly small and $\vec{E}$ is irrotational, the latter implying $\vec{E} = -\vec{\nabla}\phi$ with ϕ being the electric potential, Eq. 1 simplifies to

$$\frac{\vec{j}}{\sigma} = -\vec{\nabla}\phi - S \cdot \vec{\nabla}T. \qquad (2)$$

Considering any arbitrary temperature distribution in a medium of uniform composition in Eq. 2 shows that no current will flow because $S \cdot \vec{\nabla}T$ is also irrotational. This is due to S being a function of T only, a consequence of which is that $\vec{\nabla}S \times \vec{\nabla}T$ vanishes. In order to have thermoelectric current flowing, $\vec{\nabla}S$ and $\vec{\nabla}T$ must not be parallel. This is, in general, achieved by a spatially varying composition.

Although these basics of TEMC are known for a long time and, moreover, thermoelectromagnetic pumps have been patented and developed starting in the middle of the fifties [2–5], embodiments for an effective stirring of a liquid metal pool are badly missing. This prompted us to perform an experimental study on TEMC configurations which are concerned with the case that was termed by Shercliff as "the extreme case when the composition and S vary discontinuously across an interface along which T varies" [1]. Besides a sound direct conversion between thermal and electric energy, thermoelectromagnetic stirring is probably a likewise attractive application of the Seebeck effect. Whenever there is a freedom to use electrically conducting walls in metallurgy or, to be more precise, in any industrial process involving liquid metals, TEMC may become a most efficient and cheap tool since the necessary temperature gradient is often intrinsic to the process. To quote a few, the tin baths in both soldering machines and float glass production are alluded to as well as processing of magnesium in stainless steel containers.

The naturally arising question at this stage would be that about mass production of aluminium or even steel. Albeit being far beyond the scope of the present paper, it is worth noting that crucible walls are not necessarily to be made from metal in order to achieve a noticeable circulation of thermoelectric current. Other classes of materials exist, e. g. some semiconductors, which outperform metals by far with respect to the Seebeck coefficient. Their drawback on the other hand is, in general, a much lower electrical conductivity. However, as both Seebeck coefficient and conductivity determine the strength of the thermoelectric current, materials are

available that exhibit an overall figure of merit unreachable for any metal–metal combination. Among the most prominent examples one finds tellurides and boron-rich substances. Introductory reading to this topic is to be found in [6, 7].

2. EXPERIMENTAL SETUP

While the necessary temperature gradient $\vec{\nabla}T$ in a square box was obtained by heating and cooling, respectively, of two opposing massive copper side walls, utilizing a nickel plate having the relatively high thermoelectric power of $S_{\mathrm{Ni}} = -15\mu\mathrm{V/K}$ for the bottom established the material discontinuity with respect to the liquid metal layer in the first setup. Here, also both other side walls parallel to $\vec{\nabla}T$ were made from copper to simplify matters. Some parasitic Ohmic losses are then to be expected owing to the high ratio of electrical conductivities between those walls and the melt. Preferably, all joints should be weldable and the four side walls should be made of the same material for the ease of construction. So it made sense to deal with a potential industrial configuration yet at the stage of laboratory experiments. If TEMC stirring shows up to work in a *downgraded* setup with loss of current, it will work more than ever in an optimised configuration. In the apparatus with the electromagnet, the side walls parallel to $\vec{\nabla}T$ were however replaced with glass for the additional reason of being of more generic nature. Note that fused silica stands temperatures comparable to that of copper.

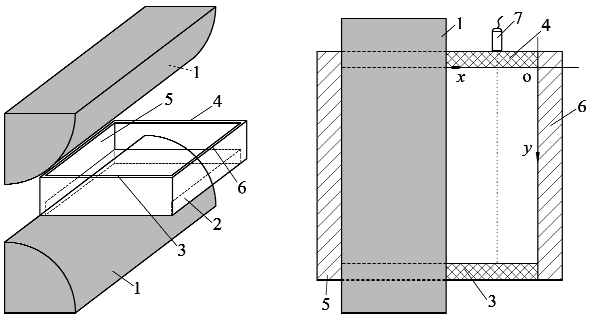

Fig. 1. Sketch of the second experimental setup in perspective (left) and top view (right). 1: pole shoes, 2: constantan or nichrome bottom, 3&4: front and rear insulating side walls, and 5&6: cooled and heated isothermal side walls, respectively. The ultrasonic sensor (7) can be traversed along the rear wall.

The task formulation of a marked TEMC may be accomplished with a strong inhomogeneity of the magnetic flux density $\vec{B}$, which was fulfilled with a $50 \times 20 \times 8\,\mathrm{mm}^3$ permanent magnet made from cobalt-samarium in the first setup. With the direction of magnetisation along the shortest side, it produced $B = 270\,\mathrm{mT}$ at its surface. Sizes of the container were $\mathrm{length} = \mathrm{width} = 15\,\mathrm{cm}$, and the filling height of the melt was always $1.5\,\mathrm{cm}$. GaInSn ($T_{\mathrm{melt}} = 10\,^{\circ}\mathrm{C}$) was chosen as the melt under investigation mainly for the reason of its thermo-emf $S_{\mathrm{GaInSn}} = -0.55\mu\mathrm{V/K}$ differing not that much from $S_{\mathrm{Cu}} = -2\mu\mathrm{V/K}$ of the copper walls. For a figure and a more detailed description of the experiment [8] is referred to. The second quadratic container used in combination with the electromagnet was a little bit smaller; the length of 12 cm was accounted for by adjusting $\vec{\nabla}T$accordingly. Figure 1 depicts the experimental arrangement and the shape of the pole shoes. In order to enhance TEMC, bottom materials with even higher absolute values of S were employed. $S_{\mathrm{constantan}} = -35\mu\mathrm{V/K}$ is probably the highest value that can be found among metals, and $S_{\mathrm{nichrome}} = 25\mu\mathrm{V/K}$ provides also the complementary case. Note that these materials differ significantly from nickel, the latter being ferromagnetic, which has a significant influence on the distribution of $\vec{\nabla}B$.

Numerical simulations were performed with the commercial solver Maxwell (Ansoft Corp.) showing that $\vec{\nabla}B$ is almost perpendicular to the bottom of the first container at least within the lower part of the metallic melt layer, as was to be expected because of the ferromagnetic nickel. The pole shoes used in the second setup produce a field with a prominent vertical component. Measurements performed with a 3-axis Gauss meter (Lakeshore, model 460) agreed nicely with the computations. For the following considerations, it is thus sufficient to restrict to B_z.

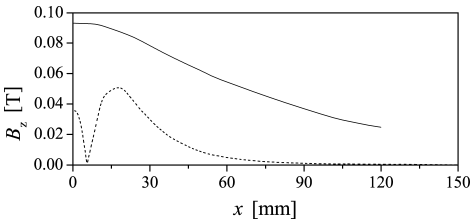

Fig. 2. Dependence of B_z at the solid–liquid interface on the position between the hot and the cold wall. Dashed line: permanent magnet, solid line: field produced by the electromagnet.

Besides observing the motion at the melt surface, local flow measurements were performed. An ultrasonic Doppler velocimeter (UDV) was used to acquire instantaneous velocity profiles along the sound beam. Takeda described the principle of operation of UDV, which is based on the pulsed echo technique, in his pioneering work [9]. A time of flight measurement of an ultrasonic burst determines the location of a scattering particle within the fluid, and the difference in time of flight measurements for consecutive bursts is a measure for the velocity of the particle travelling together with the fluid. Among others, a demonstration of the ability of UDV to work for liquid metals may be found in

[10]. No seeding of particles is required for the GaInSn under investigation. Since this melt is prone to oxidation, mixed in oxide agglomerates from the surface are sufficient for a reliable UDV echo signal.

3. RESULTS AND DISCUSSION

In a first series of experiments, the permanent magnet was located with its long side aligned to the cold wall. Under the assumption of a homogeneous thermoelectric current between the isothermal walls, the Lorentz force is directed along the wall while diminishing with increasing distance to that wall. The flow structure expected to develop thus is a recirculation in the horizontal plane: driven by the force acting in the vicinity of the wall and closing elsewhere in the liquid metal volume. Characteristic velocities v obtained with UDV measurements depended linearly on ΔT, which accords to the dimensionless parameter

$$Te = \frac{\sigma \Delta S B \Delta T l^2}{\rho \nu^2} \tag{3}$$

proposed by Gorbunov [11]. Te, l, ρ, and ν are the dimensionless number measuring the strength of TEMC, a characteristic length of the system, density, and kinematical viscosity. A typical value of the velocity for, e.g., $\Delta T = 50\,\mathrm{K}$ was $v = 70\,\mathrm{mm/s}$ clearly demonstrating the dominance of TEMC over buoyancy, the latter having produced a velocity of $5\,\mathrm{mm/s}$, only.

An entire velocity section along the propagation direction of the ultrasonic beam in conjunction with scanning the sensor in the perpendicular direction yields area-wide results, from which a stream function may be calculated. Such evaluation for the magnet being aligned at the left isothermal wall is shown in Fig. 3. It agrees nicely with the expected flow structure of a single convection cell penetrating the container entirely with the eye moved off centre toward the source of motion. Although the flow was relatively stable to the appearance of observation with the naked eye, velocities in the range of several $\mathrm{cm/s}$ indicated that the flow was not laminar. The plot of instantaneous local velocities in Fig. 4 clearly shows that the flow was indeed turbulent.

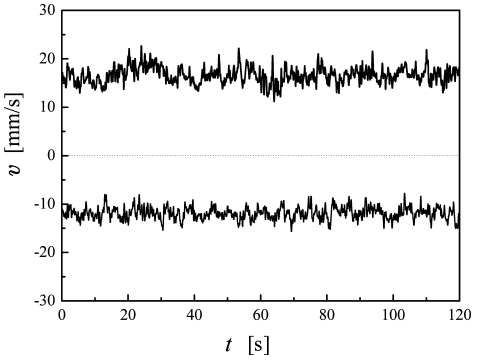

Fig. 4. Time series of the local velocity at two selected locations in configuration one. The plot corresponds to the single cell depicted in Fig. 3 with the magnet at the wall.

If the magnet is located above the centre of the container, a convective pattern consisting of four cells is to be expected from the distribution of the thermoelectromagnetic body force. Also in this configuration, the corresponding stream functions measured by scanning the UDV sensor in the second series of experiments fully supported the expectations of four vortices with diagonally opposing cells having the same rolling direction (c. f. Fig. 5). Without mention of details, which would lengthen the paper significantly while being not necessary for the scope here, it is stated that accompa-

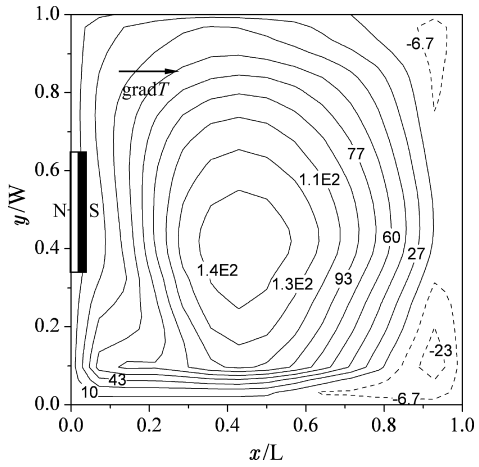

Fig. 3. Stream function in configuration one calculated from area-wide UDV measurements in the case that the magnet is located at the cold wall.

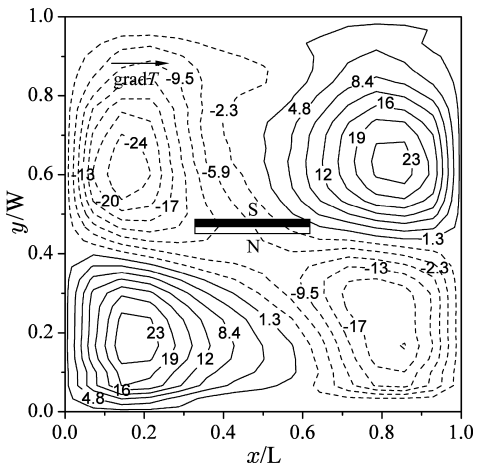

Fig. 5. Multi-cellular pattern in configuration one in the case that the magnet is centered above the container.

nying numerical results obtained for the Lorentz force and the rotor thereof supported the experimental findings with respect to the convective patterns.

Because the boundaries between the convection cells were not rigid, the system with the magnet above the center likely was the more unstable one. Free boundaries are potential sources of instability in many fluid-dynamical systems. Despite the temperature difference in the case of the centered magnet was $10\,\mathrm{K}$ higher than in the case of the single cell, mean velocities decreased distinctly whereas the turbulence was significantly intensified (see Fig. 6). The flow was characterized by oscillations of the mean flow eddies, which could have been either movement of the vortices' eyes and/or growth and shrinkage of the vortices. Intermittence was, however, not observed in the investigated range of temperature differences. More results and an extended discussion of the configuration with the permanent magnet are to be found in [8].

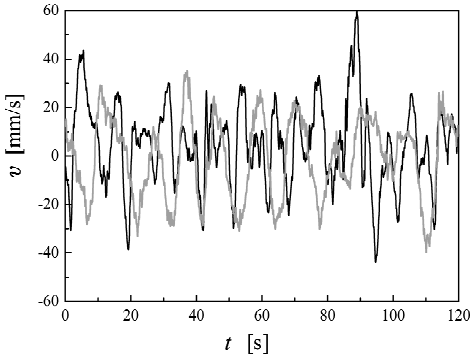

Fig. 6. Time series of the local velocity corresponding to the four-cell flow structure in Fig. 5. It is stressed that ΔT is $10\,\mathrm{K}$ lower than in Fig. 4.

The most obvious and thus first question when moving to the second setup was that about a potential mitigation of the vigour of the flow in the first container by Ohmic losses via the electrically conducting walls parallel to $\vec{\nabla}T$. The slightly different sizes were accounted for by adjusting identical $\Delta T/\mathrm{L}$, where L is the distance between the isothermal walls. Another issue with respect to contrasting the experiments is the magnetic field, of which both absolute value and gradient are important. Fig. 7 shows measurements for identical $B_\mathrm{z} = 50\,\mathrm{mT}$. For not too high field strength, which is the range wherein the damping effect of the static field remains small, these results should conform to Eq. 3 proposed by Gorbunov [11]. Since ΔS is the only parameter subject to variation, v should solely depend linearly on the emf for any $\Delta T/\mathrm{L}$. The points of the fit curves on the axis of ordinate are $v_\mathrm{Ni} = 20.7$, $v_\mathrm{nichrome} = 27.9$, and $v_\mathrm{constantan} = 49.6\,\mathrm{mm/s}$. v_Ni has to be corrected to $32.3\,\mathrm{mm/s}$ for the different characteristic length. Even though there were certainly Ohmic losses in the experiments with the copper walls parallel to $\vec{\nabla}T$, the ratio $(v/\Delta S)_\mathrm{Ni} = 2.2\mathrm{mm}\cdot\mathrm{K}/(\mu\mathrm{V}\cdot\mathrm{s})$ is much to high compared to the values of 1.1 and 1.4 for nichrome and constantan, respectively. This suggests that $\vec{\nabla}B$ should be included in a scaling law since this gradient is much steeper for the permanent magnet above a ferromagnetic bottom (c. f. Fig. 2).

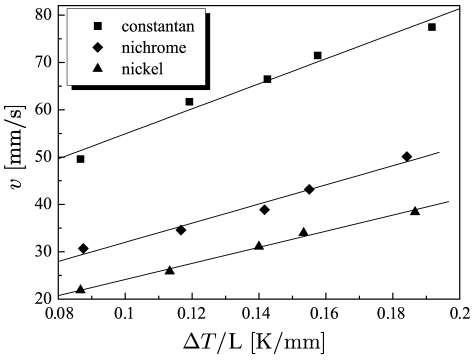

Fig. 7. Comparison of the dependence of the characteristic velocity v on the temperature drop $\Delta T/\mathrm{L}$ between the cold and the hot wall obtained in both containers having constantan and nichrome bottoms, respectively, and the box with the nickel bottom. All measurements were done at the location of maximum velocity within the container.

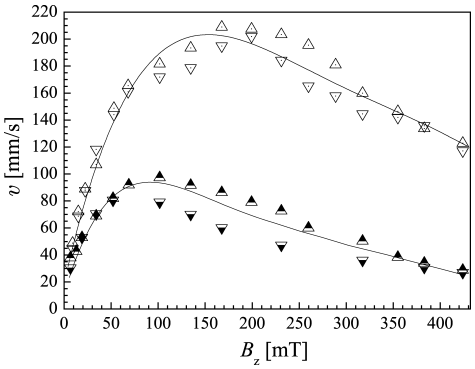

Fig. 8. Comparison of the dependence of the characteristic velocity on the vertical component of $\vec{B}$ obtained in the container with constantan bottom at $\Delta T = 30$ and $60\,\mathrm{K}$.

Fig. 8 shows four series, two for $\Delta T = 30$ and $60\,\mathrm{K}$, each, wherein B_z was varied. Despite the quite long sampling time exceeding ten minutes and comprising more than 12000 readings per measurement, the data show a significant scatter predominantly in the range of medium field strength. Moreover, there seems to be a systematic deviation within each pair. However, the also damping influence of the flow driving magnetic field is clearly demonstrated. The threshold above which braking overcomes impelling flow depends obviously on ΔT, which was not necessarily expected.

To the best of our knowledge first results on the turbulence characteristics in a thermoelectromagnetically driven flow are presented in Fig. 9. The series covered six equidistant measurements in the range from $\Delta T = 10$ to $60\,\mathrm{K}$ at $B_z = 50\,\mathrm{mT}$, not all of them are shown in the graph. Those not depicted exhibit the same characteristics of an energy spectrum gouverned by homogeneous isotropic turbulence.

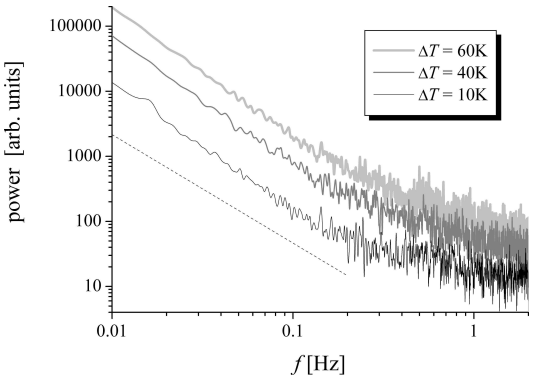

Fig. 9. Turbulence spectra for three selected temperature differences calculated from UDV measurements of the velocity component in y-direction close to the cold wall where this velocity component is maximum ($x = 10\,\mathrm{mm}$, $10 \le y \le 75\,\mathrm{mm}$; y varies with ΔT). The straight dashed line represents the case of homogeneous isotropic turbulence $E(f) \propto f^{-5/3}$.

4. SUMMARY

Thermoelectromagnetic convection (TEMC) was studied in square melt layers heated differentially in the horizontal direction. While the origin of flow is an electro-motive force, the crux of the experiments was establishing a high differential Seebeck coefficient between bottom material and the melt. Two case studies were realized: a somehow generic one with a two-dimensional distribution of the magnetic field $\vec{\nabla}B$ having a gradient in direction of the temperature difference, only, and the other one having a full 3D distribution of B. The main findings obtained with ultrasonic flow measurements are: (i) strong fluid motion suitable for metallurgical tasks is accomplishable, (ii) the vigour of the flow scales reasonably with ΔS, B, and ΔT as proposed by Gorbunov [11], (iii) at high values of B, the damping impact of the static field outbalances its flow driving effect, and (iv) $\vec{\nabla}B$ co-determining the magnitude of the rotor of the Lorentz force may become quite important. TEMC turbulence characteristics are seemingly classical, i. e. homogeneous and isotropic obeying the celebrated energy relation with its exponential $-5/3$-dependence of the kinetic energy on frequency.

ACKNOWLEDGEMENT
This work was supported by Deutsche Forschungsgemeinschaft in the framework of the collaborative research centre SFB 609 entitled "Electromagnetic Flow Control in Metallurgy, Crystal Growth, and Electrochemistry."

References

[1] J. A. SHERCLIFF. Thermoelectric magnetohydrodynamics. *J. Fluid Mech.*, Vol. 91 (1979), pp. 1917–1928.

[2] K. F. SCHOCH. An experimental liquid metal thermoelectric electro-magnetic pump – heat exchanger. *Report No. R56GL94*, General Electric Company, San Jose, CA, USA (1956).

[3] L. B. VANDENBERG. Heat exchanger pump. *US patent No. 2,748,710* (1956).

[4] S. R. ROCKLIN. Thermoelectric pump. *US patent No. 3,116,693* (1964).

[5] M. A. PERLOW, H. M. DIECKAMP. Thermoelectric pump. *US patent No. 3,288,070* (1966).

[6] A. F. IOFFE. Semiconductor Thermoelements and Thermoelectric Cooling. *Infosearch Limited, ISBN 0-8508-6039-3* (1957).

[7] H. WERHEIT. Thermoelectric Properties of Boron-Rich Solids and their Possibilities of Technical Application. *Proc. Int. Conf. on Thermoelectrics*, Aug. 2006, Vienna, Austria.

[8] X. ZHANG, A. CRAMER, G. GERBETH. Model experiments on macroscopic thermoelectromagnetic convection. *Magnetohydrodynamics*, Vol. 45/1 (2009), pp. 25–42.

[9] Y. TAKEDA. Development of an ultrasound velocity profile monitor. *Nucl. Eng. Des.*, Vol. 126 (1993), pp. 277–284.

[10] A. CRAMER, C. ZHANG, S. ECKERT. Local flow structures in liquid metals measured by ultrasonic Doppler velocimetry. *Flow Meas. Instrum.*, Vol. 15 (2004), pp. 145–153.

[11] L. A. GORBUNOV. Effect of thermoelectromagnetic convection on the production of bulk single-crystals consisting of semiconductor melts in a constant magnetic field. *Magnetohydrodynamics*, Vol. 23/4 (1987), pp. 400–407.